Arl8/ARL-8 functions in apoptotic cell removal by mediating phagolysosome formation in *Caenorhabditis elegans*

Ayaka Sasaki[a], Isei Nakae[a], Maya Nagasawa[a], Keisuke Hashimoto[a], Fumiko Abe[a], Kota Saito[a], Masamitsu Fukuyama[a], Keiko Gengyo-Ando[b,c,*], Shohei Mitani[b,c], Toshiaki Katada[a], and Kenji Kontani[a]

[a]Department of Physiological Chemistry, Graduate School of Pharmaceutical Sciences, University of Tokyo, 7-3-1 Hongo, Bunkyo-ku, Tokyo 113-0033, Japan; [b]Department of Physiology, School of Medicine, Tokyo Women's Medical University, 8-1 Kawada-cho, Shinjuku-ku, Tokyo 162-8666, Japan; [c]Core Research for Evolutional Science and Technology, Japan Science and Technology Agency, Kawaguchi, Saitama 332-0012, Japan

ABSTRACT **Efficient clearance of apoptotic cells by phagocytes is important for development, tissue homeostasis, and the prevention of autoimmune responses. Phagosomes containing apoptotic cells undergo acidification and mature from Rab5-positive early to Rab7-positive late stages. Phagosomes finally fuse with lysosomes to form phagolysosomes, which degrade apoptotic cells; however, the molecular mechanism underlying phagosome–lysosome fusion is not fully understood. Here we show that the *Caenorhabditis elegans* Arf-like small GTPase Arl8 (ARL-8) is involved in phagolysosome formation and is required for the efficient removal of apoptotic cells. Loss of function of *arl-8* results in the accumulation of apoptotic germ cells. Both the engulfment of the apoptotic cells by surrounding somatic sheath cells and the phagosomal maturation from RAB-5- to RAB-7-positive stages occur in *arl-8* mutants. However, the phagosomes fail to fuse with lysosomes in the *arl-8* mutants, leading to the accumulation of RAB-7-positive phagosomes and the delayed degradation of apoptotic cells. ARL-8 localizes primarily to lysosomes and physically interacts with the homotypic fusion and protein sorting complex component VPS-41. Collectively our findings reveal that ARL-8 facilitates apoptotic cell removal in vivo by mediating phagosome–lysosome fusion during phagocytosis.**

Monitoring Editor
Tamotsu Yoshimori
Osaka University

Received: Aug 27, 2012
Revised: Feb 19, 2013
Accepted: Mar 7, 2013

INTRODUCTION

Apoptosis, or programmed cell death, is a genetically regulated process of cell suicide. Under normal conditions, apoptotic cells are recognized and degraded by phagocytes (e.g., macrophages) before they release potentially toxic materials. Defective clearance of apoptotic cells can thus lead to various diseases, including autoimmune disorders (Elliott and Ravichandran, 2010). Phagocytic degradation of apoptotic cells is controlled by mechanisms that are well conserved from the nematode *Caenorhabditis elegans* to humans (Fadeel, 2003). *C. elegans* is a useful genetic system in which to study the mechanism controlling apoptotic cell phagocytosis (Reddien and Horvitz, 2004; Lettre and Hengartner, 2006). Two conserved signaling pathways have been proposed to mediate the recognition and internalization of apoptotic cells. In one pathway, the engulfment receptor CED-1, together with CED-7 (an ATP-binding cassette transporter), functions upstream of CED-6 (a phosphotyrosine-binding domain–containing adaptor protein) to regulate the recognition of apoptotic cells and transduce engulfing signals (Liu and Hengartner, 1998; Wu and Horvitz, 1998; Zhou *et al.*, 2001). In

This article was published online ahead of print in MBoC in Press (http://www.molbiolcell.org/cgi/doi/10.1091/mbc.E12-08-0628) on March 13, 2013.

*Present address: Saitama University Brain Science Institute, 255 Shimo-Okubo, Sakura-ku, Saitama 338-8570, Japan.

Address correspondence to: Kenji Kontani (kontani@mol.f.u-tokyo.ac.jp).

Abbreviations used: AO, acridine orange; DIC, differential interference contrast; GFP, green fluorescent protein; RNAi, RNA interference.

© 2013 Sasaki *et al.* This article is distributed by The American Society for Cell Biology under license from the author(s). Two months after publication it is available to the public under an Attribution–Noncommercial–Share Alike 3.0 Unported Creative Commons License (http://creativecommons.org/licenses/by-nc-sa/3.0).

"ASCB®," "The American Society for Cell Biology®," and "Molecular Biology of the Cell®" are registered trademarks of The American Society of Cell Biology.

the other pathway, the engulfment receptor PSR-1 acts upstream of the signaling proteins CED-2/CrkII, CED-5/Dock180, and CED-12/ELMO1 to activate CED-10/Rac1; this cascade leads to actin remodeling, which drives the growth of membrane pseudopods to enclose apoptotic cells (Fadok *et al.*, 2000; Wang *et al.*, 2003; Kinchen *et al.*, 2005).

The internalized apoptotic cells are enclosed within membrane-bound compartments called phagosomes. Phagosomes undergo a "maturation process" that involves recruitment of early/late endosomal compartments and V-ATPases for acidification (Desjardins *et al.*, 1994; Henry *et al.*, 2004). The Rab GTPases Rab5 and Rab7 are sequentially recruited to phagosomes to coordinate early-to-late phagosome maturation (Duclos *et al.*, 2000; Roberts *et al.*, 2006; Seto *et al.*, 2011). Rab5 promotes phagosomal fusion with early endosomes and regulates phagosome conversion to a Rab7-positive stage (Vieira *et al.*, 2003). Studies in *C. elegans* identified several Rab GTPases as critical regulators of phagosome maturation (Kinchen *et al.*, 2008; Lu *et al.*, 2008; Mangahas *et al.*, 2008; Yu *et al.*, 2008; Guo *et al.*, 2010; Kinchen and Ravichandran, 2010). The transition of phagosomes from the RAB-5 (Rab5)- to the RAB-7 (Rab7)-positive stage is regulated by the SAND-1 (Mon1)/CCZ-1 (Ccz1) complex (Kinchen and Ravichandran, 2010): GTP-bound RAB-5 interacts with the SAND-1/CCZ-1 complex, and the resultant RAB-5/SAND-1/CCZ-1 complex then facilitates RAB-7 activation/recruitment by dislodging GDP-bound RAB-7 from its complex with the GDP-dissociation inhibitor (GDI). RAB-7 is required for phagosome–lysosome fusion, which forms the phagolysosomes in which apoptotic cells are degraded by lysosomal hydrolytic enzymes (Kinchen *et al.*, 2008; Yu *et al.*, 2008). Studies suggested that the homotypic fusion and vacuolar protein sorting (HOPS) complex components may function downstream of RAB-7 and be involved in phagosome–lysosome fusion (Kinchen *et al.*, 2008; Yu *et al.*, 2008; Akbar *et al.*, 2011). The HOPS complex, originally characterized in yeast as a factor in vacuolar fusion, consists of six subunits (a core of four subunits, VPS-11, -16, -18, and -33, with two accessory subunits, VPS-39 and -41). In yeast, the HOPS complex is an effector of Ypt7p (yeast Rab7) and binds the vacuolar soluble *N*-ethylmaleimide–sensitive factor attachment protein receptors (SNAREs) to drive vacuole fusion (Nickerson *et al.*, 2009; Wickner, 2010; Epp *et al.*, 2011).

Arl8 is a small GTPase that is highly conserved among multicellular organisms and localizes primarily to the lysosomes (Bagshaw *et al.*, 2006; Hofmann and Munro, 2006; Nakae *et al.*, 2010). Previous studies showed that Arl8 is involved in lysosomal movement along microtubules (Bagshaw *et al.*, 2006; Hofmann and Munro, 2006) and endocytic traffic to lysosomes (Nakae *et al.*, 2010). Arl8 was shown to interact with SifA and kinesin-interacting protein (SKIP), thereby recruiting kinesin-1 to lysosomes to facilitate lysosome migration toward the cell periphery (Rosa-Ferreira and Munro, 2011). In the context of microtubule-dependent membrane transport, *C. elegans* Arl8 (ARL-8) facilitates the axonal transport of presynaptic cargoes in neurons (Klassen *et al.*, 2010). A recent article reported an unexpected role of Arl8 in *Tobmorius* RNA replication in *Arabidopsis thaliana* (Nishikiori *et al.*, 2011).

In the present study, we identified ARL-8 as a critical component for efficient phagocytic degradation of apoptotic germ cells in *C. elegans*. We found that an *arl-8* deletion mutant exhibited an accumulation of apoptotic germ cells. Apoptotic cells were engulfed by somatic sheath cells (large phagocytic cells) in the *arl-8* mutants; however, degradation of the apoptotic cells was severely impaired. In *arl-8* mutants, phagosomes containing apoptotic cells were arrested in a RAB-7–positive stage. Time-lapse imaging of live animals revealed that the fusion of lysosomes to phagosomes is defective in *arl-8* mutants. ARL-8 localized primarily to lysosomes and physically interacted with the HOPS complex component VPS-41. We therefore propose that *arl-8* acts to clear apoptotic cells by mediating phagolysosome formation.

RESULTS

arl-8 is required for cell corpse removal in the adult hermaphrodite gonad

In *C. elegans*, approximately half of the hermaphrodite germ cells undergo apoptosis and are phagocytosed by surrounding somatic sheath cells for degradation by lysosomal enzymes (Gumienny *et al.*, 1999). We previously reported that *C. elegans* ARL-8 localizes primarily to lysosomes and mediates delivery of endocytosed macromolecules to the lysosomes in macrophage-like coelomocytes (Nakae *et al.*, 2010). We found that *arl-8(tm2504)*, a strong loss-of-function mutant (Nakae *et al.*, 2010), exhibited an increased number of cell corpses in the adult gonad arms (Figure 1A, arrows). We scored cell corpses in one gonad arm of wild-type and *arl-8* mutant animals every 12 h after the L4 stage; the number of cell corpses increased progressively in an age-dependent manner in *arl-8* mutants (Figure 1B). There was no apparent difference between the wild-type and *arl-8* mutant animals in the frequency of cell death in the U-turn region of the gonad (4.4 ± 0.84 and 4.5 ± 0.74 germ cell deaths in 180 min in wild-type and *arl-8(tm2504)* animals, respectively; $n = 4$), suggesting that the increase in the number of cell corpses in *arl-8(tm2504)* animals was not caused by elevated germ cell apoptosis. We next analyzed cell corpse duration to investigate whether *arl-8(tm2504)* mutants are defective in cell corpse removal. Most cell corpses were degraded within 50 min after their appearances in the wild type, whereas they persisted for more than 100 min in *arl-8(tm2504)* animals (Figure 1D), indicating that the clearance of cell corpses is impaired in *arl-8(tm2504)* animals. The *arl-8(tm2504)* persistent cell corpse phenotype was significantly rescued by expression of *arl-8::venus* under the *ced-1* promoter, which drives gene expression specifically in the engulfing sheath cells (Figure 1C). These results suggest that *arl-8* is required for the efficient removal of apoptotic cells by sheath cells. It remains to be determined whether *arl-8(tm2504)* animals are defective also for the removal of embryonic apoptotic cells, since the homozygous embryos from *arl-8(tm2504)* homozygous hermaphrodites arrest in early embryonic stages before programmed cell death is induced (unpublished data).

Phagosomes containing cell corpses are arrested at an RAB-7–positive stage in *arl-8* mutants

Apoptotic germ cells are engulfed by sheath cells and subsequently degraded inside phagosomes. We first investigated whether the apoptotic cells were engulfed by the sheath cells in *arl-8* mutants using acridine orange (AO), which preferentially stains acidic compartments and can be used to label the internalized cell corpses in living cells (Gumienny *et al.*, 1999; Lu *et al.*, 2008; Xiao *et al.*, 2009). Most cell corpses in *arl-8* mutants were stained by AO (Figure 2A), indicating that the cell corpses were engulfed by the sheath cells. Phagosomal acidification in *arl-8* mutants was also confirmed by LysoTracker Red staining (Figure 2B). We next analyzed the phagosomal maturation of *arl-8* mutants by examining the recruitment of Rab GTPases to the phagosomes. Studies showed that the phagosomes recruit RAB-5 and RAB-7 sequentially to their membranes: whereas RAB-5 is recruited transiently to early phagosomes, RAB-7 is present on phagosomes at late stages of phagosome maturation (Kinchen *et al.*, 2008; Kinchen and Ravichandran, 2010; Yu *et al.*, 2008). Time-lapse analysis showed that GFP::RAB-5 was recruited to

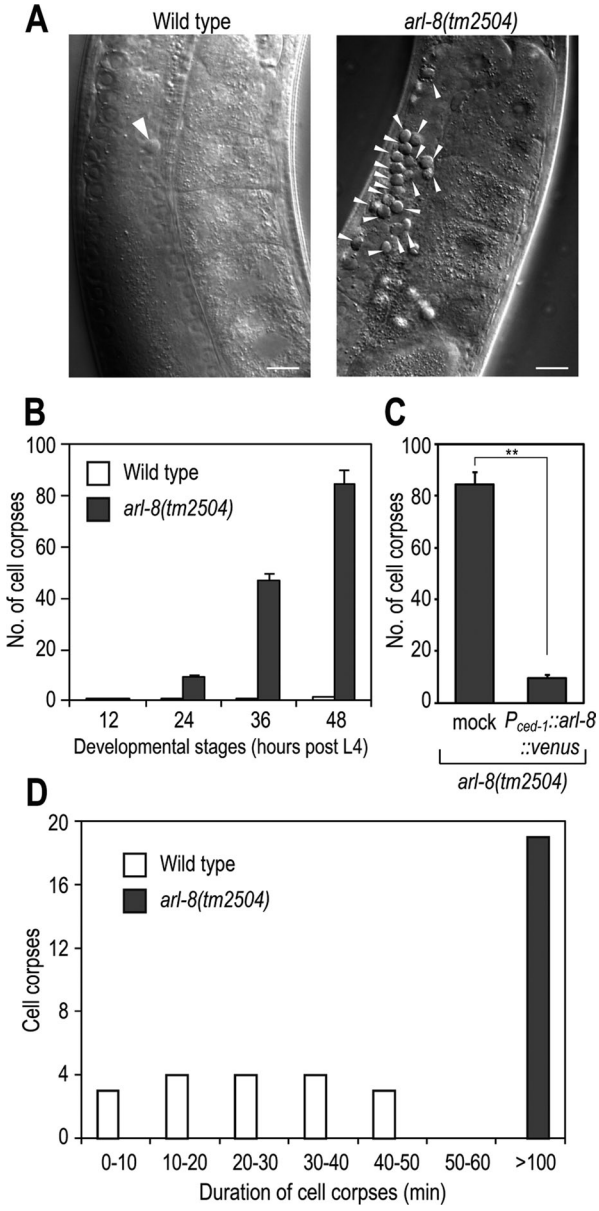

FIGURE 1: *arl-8(tm2504)* mutants are defective in the removal of germ cell corpses. (A) Nomarski images of gonad arms in wild-type or *arl-8(tm2504)* adult hermaphrodites 48 h after the L4 larval stage. Germ cell corpses are marked with arrowheads. Bars, 10 μm. (B) Germ cell corpses of one gonad arm from each animal were scored every 12 h after the L4 larval stage. Fifteen animals were scored for each strain, and data are expressed as mean ± SEM. (C) The increased germ cell corpse phenotype of *arl-8(tm2504)* animals was rescued by $P_{ced\text{-}1}$*::arl-8::venus*. Germ cell corpses of one gonad arm from the indicated animals were scored after the L4 larval stage. More than 10 animals were scored for each strain, and the data are expressed as mean ± SEM. $^{**}p < 0.01$ by Student's *t* test. (D) Histogram summarizing cell corpse duration the germline of the indicated animals. More than 15 cell corpses were monitored in each strain.

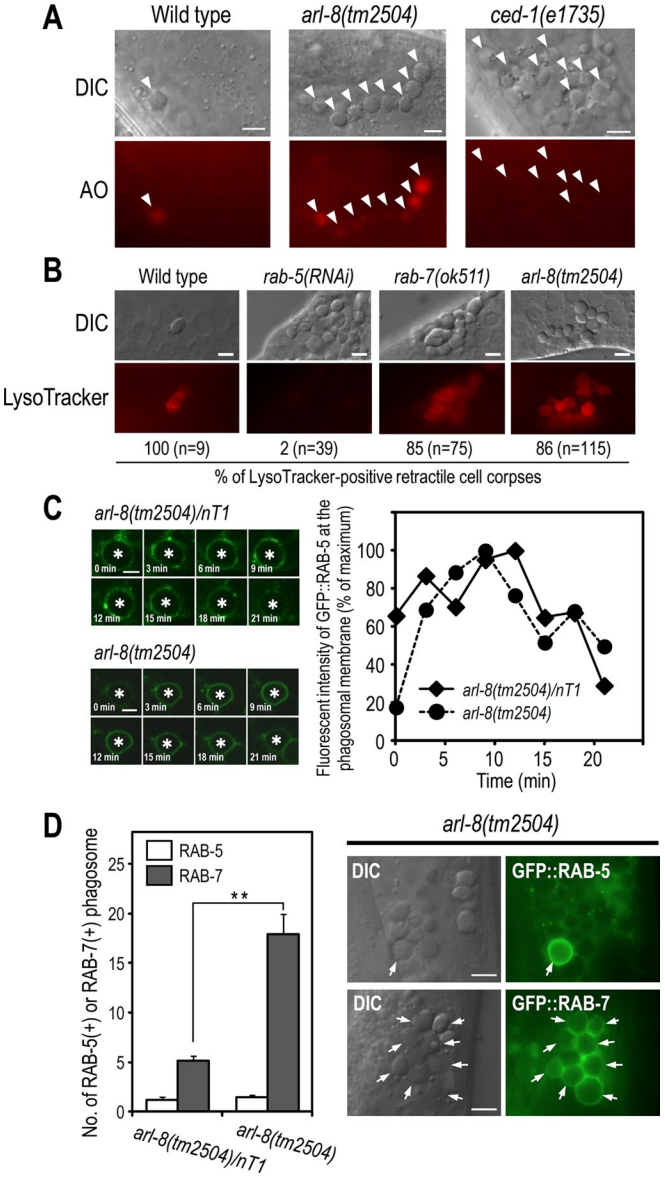

FIGURE 2: Phagosomes are arrested at an RAB-7–positive stage in *arl-8(tm2504)* mutants. (A) AO staining of germ cell corpses in the indicated animals. Germ cell corpses are marked with arrowheads. Most cell corpses were stained by AO in *arl-8(tm2504)* animals, whereas corpses were not stained in *ced-1(e1735)* animals in which cell corpses are not phagocytosed by sheath cells. Bars, 5 μm. (B) LysoTracker staining of germ cell corpses and quantitation of LysoTracker-positive cell corpses in the indicated animals. *n*, number of cell corpses scored. Bars, 5 μm. (C) Time-lapse images of GFP::RAB-5 expression at the phagosome (left) and quantitation of the fluorescence intensity (right) in *arl-8(tm2504)/nT1* (as a control) and *arl-8(tm2504)* animals. Asterisks indicate germ cell corpses. Bars, 2.5 μm. (D) Quantitation of RAB-5–positive and RAB-7–positive phagosomes in the germline of the indicated animals (left). Fifteen animals were scored for each strain, and data are expressed as mean ± SEM. $^{**}p < 0.01$ by Student's *t* test. Nomarski and fluorescence images of *arl-8(tm2504)* animals expressing GFP::RAB-5 or GFP::RAB-7 (right). Arrows indicate the germ cell corpses positive for the corresponding GFP-marker proteins. Bars, 5 μm.

nascent phagosomes in *arl-8(tm2504)* animals and detached from the phagosomes similarly to that in the control *arl-8(tm2504)/nT1* animals (Figure 2C), although the average duration of RAB-5 at phagosomes of *arl-8(tm2504)* was slightly longer than that of *arl-8(tm2504)/nT1* (39.2 ± 2.33 and 33.2 ± 1.91 min, respectively; $n = 11$). The number of RAB-5–positive phagosomes in *arl-8* mutants was comparable to that observed in the wild type, whereas the number of RAB-7–positive phagosomes increased to a great degree in *arl-8* mutants (Figure 2D). Although we cannot rule out the

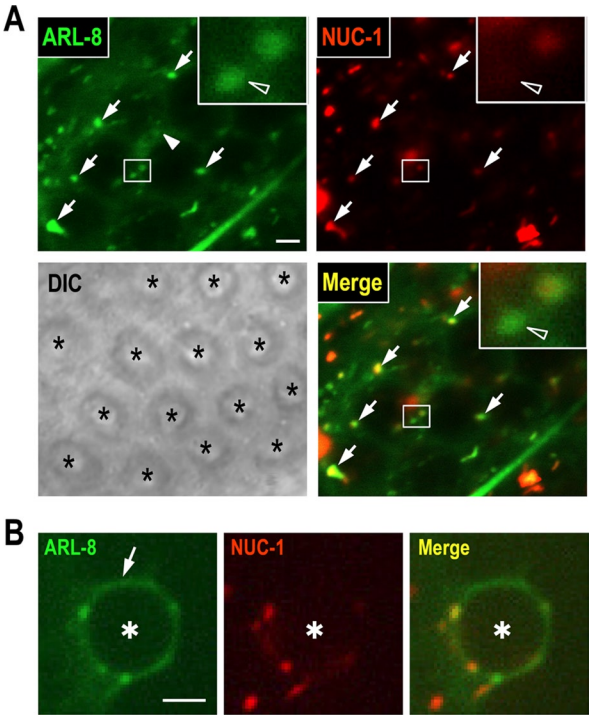

FIGURE 3: Analysis of ARL-8::GFP localization in sheath cells. (A) Fluorescence and differential interference contrast images of the gonad arm of a wild-type animal coexpressing ARL-8::GFP and NUC-1::mCherry. Asterisks indicate germ cells. ARL-8::GFP was observed in punctate structures (arrows) and cytoplasm surrounding germ cells (arrowhead). Insets, enlarged views of the areas indicated by white rectangles. The open arrowheads in the insets indicate puncta of ARL-8::GFP with little NUC-1::mCherry. Bar, 2 μm. (B) Fluorescence images of a phagosome containing a germ cell corpse (asterisk) in a wild-type animal coexpressing ARL-8::GFP and NUC-1::mCherry. ARL-8::GFP was observed at the phagosomal membrane (arrow). Bar, 2.5 μm.

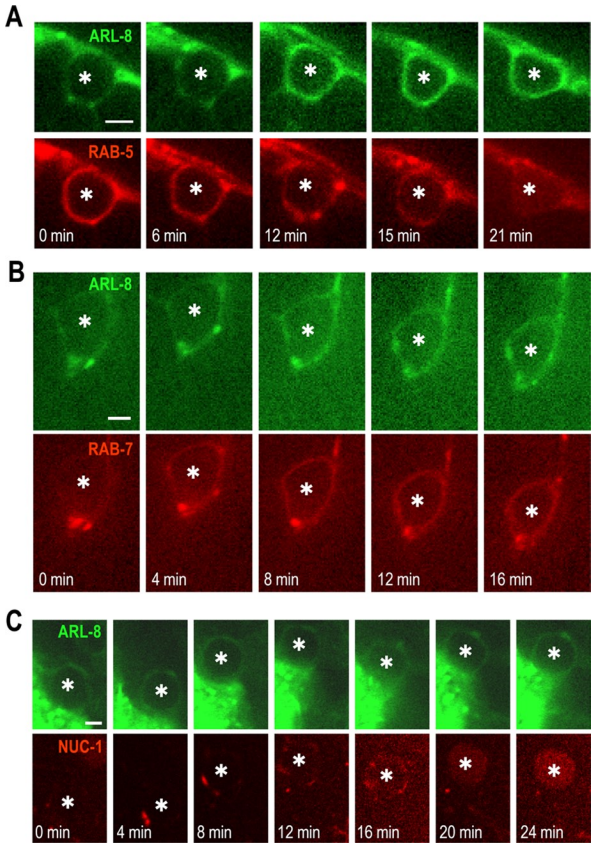

FIGURE 4: ARL-8 is recruited to phagosomes at late stages of phagosome maturation. Time-lapse images of fluorescence signal at a phagosome containing a germ cell corpse (asterisk) in a wild-type animal coexpressing ARL-8::GFP and mCherry::RAB-5 (A), ARL-8::GFP and mCherry::RAB-7 (B), or ARL-8::GFP and NUC-1::mCherry (C). Bars, 2.5 μm.

possibility that loss of *arl-8* affects early stages of phagosome maturation, these results suggest that the phagosomes of *arl-8* mutants undergo early maturation and arrest at a RAB-7–positive late stage.

ARL-8 is localized to lysosomes and recruited to phagosomes at late stages of phagosome maturation

To investigate the potential function of ARL-8 in phagosomal maturation, we analyzed the localization of ARL-8::green fluorescent protein (GFP) in sheath cells. ARL-8::GFP was detected in the punctate structures (arrows in Figure 3A) and also in the cytoplasm surrounding germ cells (arrowhead in Figure 3A). Consistent with reports showing that Arl8/ARL-8 localizes primarily to lysosomes (Bagshaw *et al.*, 2006; Hofmann and Munro, 2006; Nakae *et al.*, 2010), most ARL-8::GFP-labeled punctate structures colocalized with NUC-1::mCherry (NUC-1: a lysosomal nuclease involved in the degradation of apoptotic cell DNA; Wu *et al.*, 2000; Guo *et al.*, 2010). We observed some ARL-8::GFP-positive structures with little NUC-1::mCherry (open arrowhead in the inset of Figure 3A), suggesting that ARL-8 may also localize to other membrane compartments besides lysosomes (e.g., endosomes).

ARL-8::GFP was also detected at phagosomal membranes (arrow in Figure 3B). To investigate the dynamics of ARL-8 localization to phagosomes, we performed time-lapse imaging of transgenic animals expressing both ARL-8::GFP and mCherry::RAB-5 (an early-stage marker of phagosome maturation). ARL-8::GFP signal was only faint at the RAB-5–labeled phagosomal membranes (0 min in Figure 4A). The ARL-8 signal then proceeded to form a smooth, continuous circle, whereas the RAB-5 signal on phagosomes decreased; phagosomes converted from RAB-5 positive/ARL-8 negative to RAB-5 negative/ARL-8 positive. Next we did time-lapse analysis using transgenic animals expressing both ARL-8::GFP and mCherry::RAB-7 (a late-stage maker of phagosomal maturation), showing that the timing of ARL-8::GFP localization to phagosomes was similar to that of mCherry::RAB-7 (Figure 4B). Both ARL-8 and RAB-7 persisted on the phagosomes until degradation of phagosomal contents (unpublished data). Collectively these results indicate that ARL-8 was localized to phagosomes at late stages of phagosome maturation.

Because ARL-8::GFP was observed in both lysosomes and phagosomes, we investigated whether phagosomal localization of ARL-8 was simply a consequence of phagosome–lysosome fusion. Time-lapse analysis using transgenic animals expressing both ARL-8::GFP and NUC-1::mCherry showed that ARL-8::GFP was localized to phagosomes in which no apparent incorporation of NUC-1::mCherry was observed (0 min in Figure 4C and Supplemental Movie S1). ARL-8::GFP-labeled phagosomes then gradually fused with NUC-1::mCherry-labeled lysosomes, leading to the formation of phagolysosomes in which NUC-1::mCherry accumulated (24 min in Figure 4C). Given that ARL-8::GFP was detected in

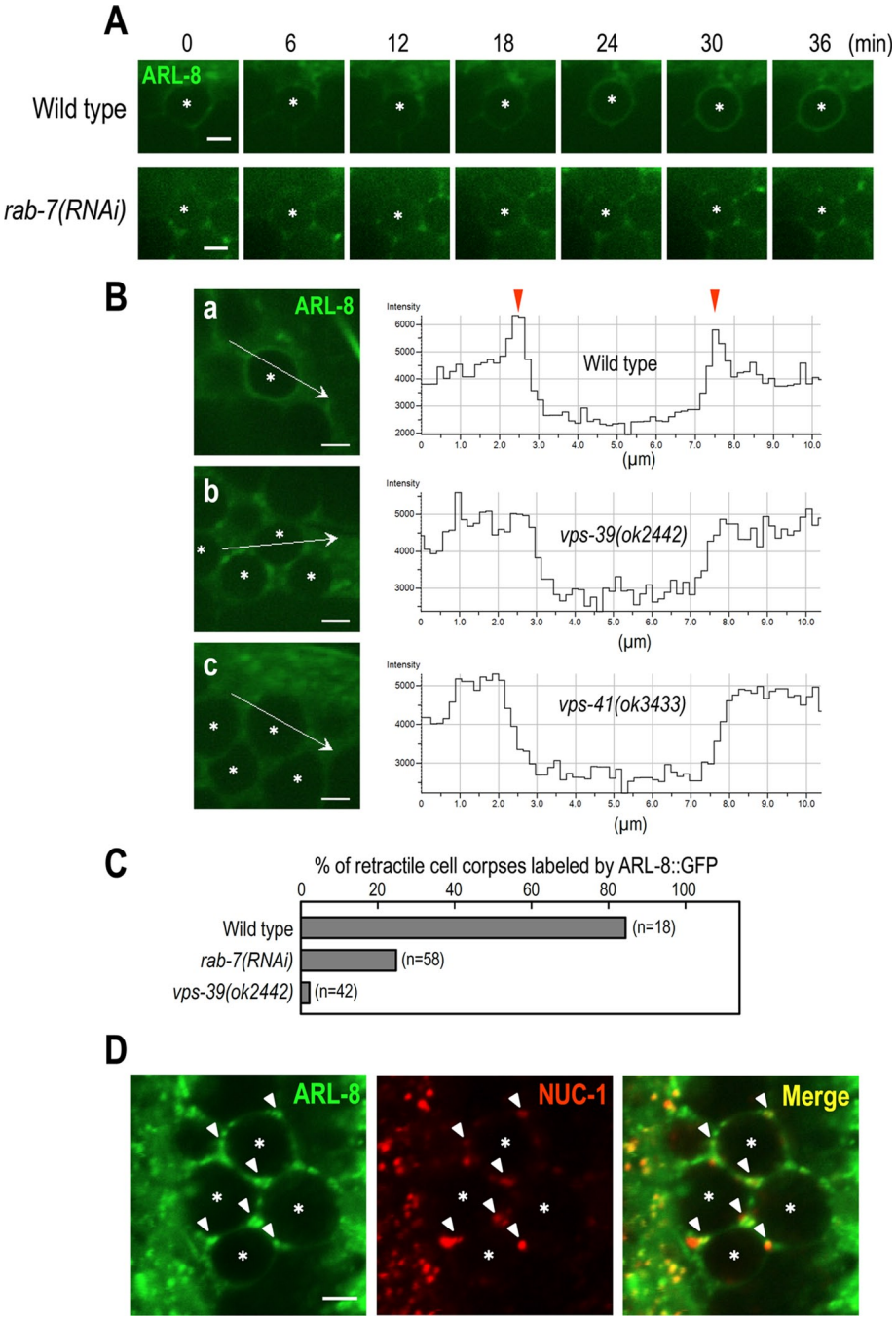

FIGURE 5: Analysis of ARL-8::GFP localization in *rab-7* and the HOPS-complex mutants. (A) Time-lapse images of ARL-8::GFP signal in the gonad of wild-type and *rab-7(RNAi)* animals. Here 0 min represents the point at which mCherry::RAB-5 (not shown) was first detected on phagosomal membranes. Asterisks indicate germ cell corpses. Bars, 2.5 μm. (B) Fluorescence images of the gonad of wild-type (a), *vps-39(ok2442)* (b), or *vps-41(ok3433)* (c) animals expressing ARL-8::GFP and line-scan quantitation of the fluorescence signal at the position indicated by the white arrow in a–c. Asterisks indicate germ cell corpses. Bars, 2.5 μm. (C) The ratio of cell corpses labeled by ARL-8::GFP in the indicated animals. *n*, number of cell corpses scored. (D) Fluorescence images of the gonad arm of *vps-39(ok2442)* coexpressing ARL-8::GFP and NUC-1::mCherry. ARL-8::GFP-labeled punctate structures colocalized with NUC-1::mCherry (arrowheads). Asterisks indicate germ cell corpses. Bar, 2.5 μm.

NUC-1::mCherry-negative compartments (Figure 3A), phagosomal localization of ARL-8::GFP may be archived not only via phagosome–lysosome fusion but also via fusion of these compartments with phagosomes before phagolysosome formation.

Localization of ARL-8 on phagosomes requires RAB-7 and the HOPS-complex subunits

Because ARL-8 colocalized with RAB-7 at phagosomal membranes, we investigated whether phagosomal localization of ARL-8 requires RAB-7. We found that ARL-8::GFP failed to localize to phagosomes in *rab-7(RNAi)* mutants and persisted as punctate fluorescence around phagosomes (Figure 5A). This result indicates that *rab-7* is required for the phagosomal localization of ARL-8. Studies suggested that the HOPS complex functions downstream of *rab-7* during phagosomal maturation: loss of function of the HOPS-complex component VPS-39 leads to the accumulation of arrested phagosomes at the RAB-7–positive stage (Kinchen *et al.*, 2008; Kinchen and Ravichandran, 2010; Akbar *et al.*, 2011). To determine whether the HOPS complex is involved in the phagosomal localization of ARL-8, we analyzed the ARL-8::GFP localization in the deletion mutants of HOPS-complex subunits VPS-39 and VPS-41. Whereas localization of ARL-8::GFP on the phagosomal membranes in wild-type animals was observed as two fluorescence peaks along the line scan (arrowheads in Figure 5B), no apparent phagosomal localization of ARL-8::GFP was observed in *vps-39(ok2422)* and *vps-41(ok3433)* animals (Figure 5B). These results indicate that both *rab-7* and the HOPS complex are required for ARL-8 localization to phagosomes. In contrast, ARL-8::GFP colocalized with NUC-1::mCherry in *vps-39(ok2422)* animals to a similar extent as in wild-type animals (Figure 5D), suggesting that ARL-8::GFP localizes to lysosomes in a HOPS complex–independent manner.

ARL-8 physically interacts with VPS-41 and is required for phagosome–lysosome fusion

We investigated whether ARL-8 can physically interact with the HOPS-complex components. Purified recombinant Flag-tagged ARL-8 proteins prebound to either GTPγS or GDP were incubated with HEK293T cell lysates containing Myc-tagged VPS-41 and then immunoprecipitated with anti-Flag M2 agarose. We found that GTPγS-bound Flag-ARL-8 preferentially associated with Myc-VPS-41 (Figure 6A), which is consistent with a report showing that GTP-bound active Arl8b binds to VPS41 in mammalian cells (Garg *et al.*, 2011). These results suggest that VPS-41 may function as an effector protein of ARL-8 in the phagocytic pathway. Finally, we investigated whether *arl-8* is required for phagolysosome formation. In wild-type animals, NUC-1::mCherry-labeled lysosomes were observed on the surface of phagosomes, and NUC-1::mCherry fluorescence then

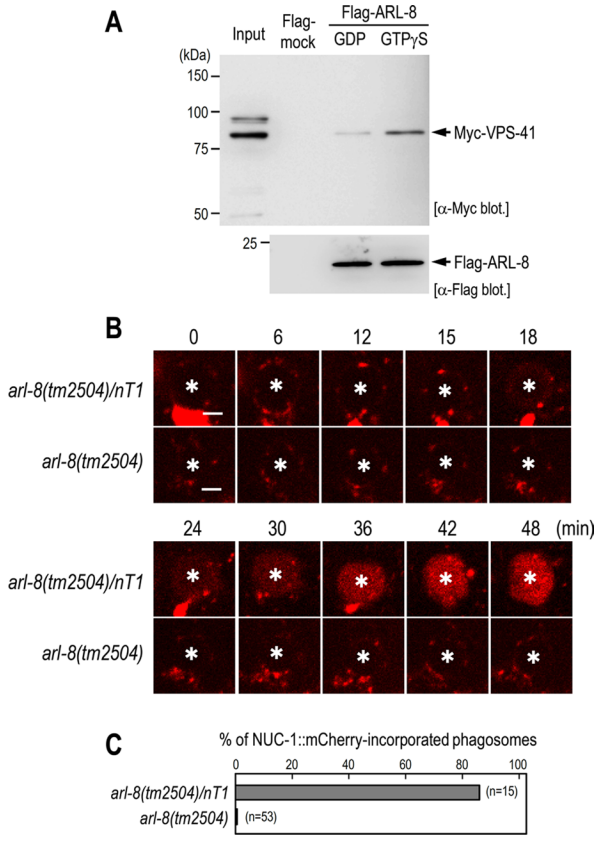

FIGURE 6: ARL-8 physically interacts with VPS-41 and is required for phagosome–lysosome fusion. (A) Pull-down assay using Flag-ARL-8 and Myc-VPS-41. Purified Flag-ARL-8 proteins preloaded with either GDP or GTPγS were incubated with HEK293T cell lysates containing Myc-VPS-41 and immunoprecipitated using anti-Flag M2 agarose. The precipitated fractions were then subjected to Western blot analysis using the indicated antibodies. (B) Time-lapse images of NUC-1::mCherry signal in the gonad of *arl-8(tm2504)/nT1* and *arl-8(tm2504)* animals. Asterisks indicate germ cell corpses. Here 0 min represents the point at which GFP::RAB-5 (not shown) was first detected on phagosomal membranes. Bars, 2.5 μm. (C) Quantitation of fusion events in the indicated animals. Data are expressed as the ratio of cell corpses that incorporated NUC-1::mCherry within 1 h after their appearance. *n,* number of cell corpses scored.

gradually increased inside the phagosomes, which likely represents phagolysosome formation via phagosome–lysosome fusion. We observed severe defects in the incorporation of NUC-1:mCherry into phagosomes of the *arl-8* mutants: NUC-1:mCherry-labeled punctate structures were observed near the phagosomes of the *arl-8* mutants, but the fluorescence failed to be incorporated into the phagosomes (Figure 6, B and C). These results suggest that phagosome–lysosome fusion is impaired in *arl-8* mutants. We tested whether loss of *arl-8* affects the morphology of lysosomes, since Arl8 and rab7 have recently been shown to be necessary for lysosome tubulation in mammalian macrophages (Mrakovic *et al.*, 2012). We found that NUC-1::mCherry-labeled tubular structures were impaired in *arl-8* mutants (Supplemental Figure S1), suggesting that *arl-8* may be involved in the formation of normal lysosomes.

DISCUSSION

The engulfment and clearance of apoptotic cells by neighboring cells or professional phagocytes is crucial to tissue homeostasis and the regulation of immune responses. In the present study, we identified *arl-8* as a novel factor essential for the efficient degradation of apoptotic cells in *C. elegans*. Deletion of *arl-8* resulted in the accumulation of apoptotic germ cells. The cell corpses were engulfed by phagocytic sheath cells in *arl-8* mutants; however, the phagosomes containing cell corpses arrested in RAB-7–positive stages and exhibited impaired cell corpse degradation. ARL-8 localized primarily to lysosomes and physically interacted with the HOPS-complex component VPS-41. Finally, the loss of *arl-8* caused defective phagosome–lysosome fusion. These results suggest that ARL-8 mediates phagolysosome formation to promote the degradation of apoptotic cells in vivo.

Phagosomes are dynamic, membrane-bound organelles that degrade a variety of particles, including potentially pathogenic microorganisms and apoptotic cells. After particle internalization, the nascent phagosome undergoes a complex maturation process involving sequential recruitment of endosomal compartments (Vieira *et al.*, 2002; Kinchen and Ravichandran, 2008). Rab5 is transiently recruited to and subsequently removed from nascent phagosomes and is required for phagosomal maturation into a later Rab7-positive stage (Duclos *et al.*, 2000; Vieira *et al.*, 2003; Roberts *et al.*, 2006; Kinchen and Ravichandran, 2010). Although the duration of RAB-5 at phagosomes was slightly longer in *arl-8* mutants than in wild type, RAB-7 was recruited to the phagosomes, indicating that phagosomes undergo the transition from early- to late-stage maturation in *arl-8* mutants. Consistent with this, the phagosomes of *arl-8* mutants were stained with acid-tropic dyes (AO and LysoTracker Red), which preferentially stain late-stage, internalized apoptotic cells. These results suggest that phagosomes are arrested at a RAB-7–positive late stage of maturation in *arl-8* mutants.

We previously showed that ARL-8 localizes primarily to lysosomes in the macrophage-like coelomocytes (Nakae *et al.*, 2010). Consistent with this, most ARL-8::GFP-labeled structures were positive for the lysosomal enzyme marker NUC-1::mCherry in sheath cells. Note that a fraction of ARL-8::GFP-labeled structures were negative for NUC-1::mCherry. ARL-8 may thus be localized also to other membrane compartments besides lysosomes (e.g., endosomes). Given that early/late endosomal components were recruited to phagosomes during phagosomal maturation (Desjardins *et al.*, 1994; Henry *et al.*, 2004) and that ARL-8::GFP was observed at phagosomes before the formation of phagolysosomes (Figure 4C), ARL-8-positive endosomes may fuse with phagosomes to form ARL-8–labeled phagosomes, which subsequently fuse with lysosomes to form phagolysosomes. Further analysis is required to determine whether the preceding association of ARL-8 with phagosomes is involved in the subsequent phagosome–lysosome fusion.

Previous studies showed that RAB-7–positive phagosomes finally fuse with lysosomes to form the phagolysosomes in which cell corpses are degraded. The molecular mechanism underlying this process is poorly understood. Studies suggested that the HOPS complex functions downstream of RAB-7 to mediate phagosome–lysosome fusion (Kinchen *et al.*, 2008; Akbar *et al.*, 2011). Given that the yeast HOPS complex is recruited to Ypt7p/Rab7 on vacuolar membranes and interacts with SNAREs required for membrane fusion, the HOPS complex may be recruited to phagosomes via RAB-7 in sheath cells and involved in phagosome–lysosome fusion. Of interest, a recent report showed that human Arl8b interacts with the HOPS-complex subunit VPS41 and is involved in the recruitment of the HOPS components to Arl8b-positive compartments (Garg *et al.*, 2011). Given that ARL-8 localized primarily to lysosomes and physically interacted with VPS-41, the HOPS complex may be recruited to

both RAB-7–positive phagosomes and ARL-8–positive lysosomes, thereby promoting fusion between phagosomes and lysosomes. Alternatively, given that phagosomal localization of ARL-8 preceded phagolysosome formation and required the HOPS-complex components, the HOPS complex may be involved in the fusion of ARL-8–positive endosomal compartments with phagosomes to promote phagosomal maturation required for the subsequent fusion with lysosomes. To test these possibilities, we tried to determine the subcellular localization of the HOPS complex in sheath cells; however, various attempts to create transgenic animals that express sufficient levels of GFP- or mCherry-fusion proteins of the HOPS components have been unsuccessful. Future studies are thus needed to clarify the functional relationships among ARL-8, RAB-7, and the HOPS complex in the phagocytic pathway.

We previously reported that ARL-8 is required for endocytic traffic to lysosomes in macrophage-like coelomocytes in *C. elegans* (Nakae *et al.*, 2010). The present study suggests that ARL-8 plays an important role in the delivery of phagocytosed cargo to lysosomes. Consistent with these findings, mammalian Arl8b was shown to be involved in the transport of various cargoes to lysosomes in macrophages (Garg *et al.*, 2011). In contrast, Arl8b was reported to be dispensable for the trafficking of endocytosed BSA to lysosomes in HeLa cells (Kaniuk *et al.*, 2011). The requirement of Arl8b for cargo trafficking to lysosomes may thus depend on cell type and/or cellular status. Uncovering the lysosomal delivery regulatory mechanism mediated by Arl8/ARL-8 may help to elucidate the spatiotemporal control of degradation of cargo molecules in lysosomes.

MATERIALS AND METHODS

Strains and genetics

Worm cultures and genetic crosses were typically performed according to standard protocols (Brenner, 1974). The N2 Bristol strain was used as the wild-type strain. Other strains used in this study are as follows: CB3203 *ced-1(e1735) I*, YB513 *arl-8(tm2504) IV/nT1*[*qIs51*](*IV;V*), VC2542 *vps-39(ok2442) V/nT1*[*qIs51*](*IV;V*), VC2784 *+/szT1*[*lon-2(e678)*] *I; vps-41(ok3433)/szT1 X*, YB1439 *arl-8(tm2504) IV/nT1*[*qIs51*](*IV;V*); *qxIs58*[$P_{ced\text{-}1}$*::lmp-1::Cherry*]; *tdEx955* [$P_{ced\text{-}1}$*::arl-8::venus*, *rol(su1006)*], YB2187 *arl-8(tm2504) IV/nT1*[*qIs51*](*IV;V*); *tdEx1504*[$P_{ced\text{-}1}$*::gfp::rab-5*, $P_{ced\text{-}1}$*::nuc-1::mCherry*, *rol-6(su1006)*], YB1468 *arl-8(tm2504) IV/nT1*[*qIs51*] (*IV;V*); *qxIs58*[$P_{ced\text{-}1}$*::lmp-1::Cherry*]; *tdEx974* [$P_{ced\text{-}1}$*::gfp::rab-5*, *rol-6(su1006)*], YB1471 *arl-8(tm2504) IV/nT1*[*qIs51*](*IV;V*); *qxIs58*[$P_{ced\text{-}1}$*::lmp-1::Cherry*]; *tdEx977* [$P_{ced\text{-}1}$*::gfp::rab-7*, *rol-6(su1006)*], YB2034 *arl-8(tm2504) IV /nT1*[*qIs51*](*IV;V*); *tdEx1385*[$P_{ced\text{-}1}$*::nuc-1::mCherry*, *rol-6(su1006)*], YB2003 *tdEx1361*[$P_{ced\text{-}1}$*::nuc-1::mCherry*, *rol-6(su1006)*], YB2036 *tdIs27*[$P_{arl\text{-}8}$*::arl-8::gfp*, *rol-6(su1006)*]; *tdEx1387*[$P_{ced\text{-}1}$*::nuc-1::mCherry*], YB1966 *tdIs27*[$P_{arl\text{-}8}$*::arl-8::gfp*, *rol-6(su1006)*]; *tdEx1332*[$P_{ced\text{-}1}$*::mCherry::rab-5*], YB2068 *tdIs27*[$P_{arl\text{-}8}$*::arl-8::gfp*, *rol-6(su1006)*]; *tdEx1418*[$P_{ced\text{-}1}$*::mCherry::rab-7*], YB2098 *vps-39(ok2442) V/nT1*[*qIs51*](*IV;V*); *tdIs27*[$P_{arl\text{-}8}$*::arl-8::gfp*, *rol-6(su1006)*], YB2270 *+/szT1*[*lon-2(e678)*] *I; vps-41(ok3433)/szT1 X; tdIs27*[$P_{arl\text{-}8}$*::arl-8::gfp*, *rol-6(su1006)*], YB2221 *vps-39(ok2442) V/nT1*[*qIs51*](*IV;V*); *tdIs27*[$P_{arl\text{-}8}$*::arl-8::gfp*, *rol-6(su1006)*]; *tdEx1534*[$P_{ced\text{-}1}$*::nuc-1::mCherry*]. The strains were maintained at 15 or 20°C. *tdIs27*[$P_{arl\text{-}8}$*::arl-8::gfp*, *rol-6(su1006)*] was isolated by ultraviolet irradiation methods (Mitani, 1995). *qxIs58*[$P_{ced\text{-}1}$*::lmp-1::Cherry*] was kindly provided by X. Wang (National Institute of Biological Sciences, Beijing, China). Germline transformation experiments were conducted by injecting various constructs with coinjection markers (Mello *et al.*, 1991).

Plasmid constructs

To generate $P_{ced\text{-}1}$*::arl-8::venus*, a 5-kb fragment of the upstream promoter region of the *ced-1* gene was amplified from genomic DNA by PCR using the primers 5′-GCGGCCGCTTGCGGCTG-CAAAAAAACAGG-3′ and 5′-GGATCCCTGGATTAGTCATACCTC-CTG-3′ and subsequently cloned into the venus-fusion expression vector pFX- *arl-8::venus*, which contains the entire coding region of the *arl-8* gene. To generate $P_{ced\text{-}1}$*::gfp::rab-7*, the entire coding region of the *rab-7* gene was amplified from genomic DNA by PCR using the primers 5′-CGGGATCCAATGTCGGGAACCAGAAA-GAAG-3′ and 5′-CGGGATCCTTAACAATTGCATCCCGAATTCTG-3′ and subsequently cloned into the GFP-fusion expression vector pKK04; this insertion was followed by the insertion of the genomic DNA fragment containing the promoter region of the *ced-1* gene. A similar strategy was used to generate $P_{ced\text{-}1}$*::gfp::rab-5* using the primer sets 5′-GCGGATCCTATGGCCGCCCGAAACG-3′ and 5′-CG-GGATCCTTATTTACAGCATGAACCCTTTTGTTGC-3′). To generate $P_{ced\text{-}1}$*::nuc-1::mCherry*, the entire coding region of the *nuc-1* gene was amplified from genomic DNA by PCR using the primers 5′-GCG-GCCGCATGGGCTTGTCTCCTGCC-3′ and 5′-GCGGCCGCATG-CACAATTATTTTGGGTTGCAA-3′ and subsequently cloned into the mCherry-fusion expression vector pFX-$P_{ced\text{-}1}$*::mCherry*, which contains the promoter region of the *ced-1* gene. To generate $P_{ced\text{-}1}$*::mCherry::rab-5* and $P_{ced\text{-}1}$*::mCherry::rab-7*, the entire coding regions of *rab-5* and *rab-7* were prepared by *Bam*HI digestion of $P_{ced\text{-}1}$*::gfp::rab-5* and $P_{ced\text{-}1}$*::gfp::rab-7*, respectively, and the resultant DNA fragments were subcloned into the *Bam*HI site of the mCherry-fusion expression vector pKK06, which contains the promoter region of the *ced-1* gene.

Quantification of cell corpses

Germ cell corpses were scored using Nomarski optics. Cell corpses in the germline meiotic region of one gonad arm were scored 12, 24, 36, and 48 h after the L4 stage. To record the duration of the cell corpses, adult animals (48 h post L4 stage) were mounted on 4% agarose pads with 2 mM levamisole in M9 medium. The gonad arm was observed under Nomarski optics manually every 5 min for 180 min. The temperature was maintained at 18–22°C during the scoring.

Acridine orange and LysoTracker staining

AO staining was performed as described previously, with minor modifications (Xiao *et al.*, 2009). Adult animals were incubated in 250 µl of M9 medium containing AO (0.14 mg/ml) and OP50 bacteria for 90 min in the dark. The stained animals were transferred to growth medium plates to recover for 1 h and then examined under fluorescence microscopy to score the AO-positive germ cell corpses. LysoTracker staining was performed as described previously, with slight modifications (Guo *et al.*, 2010). Briefly, adult animals were dissected in staining buffer (20 mM Na 4-(2-hydroxyethyl)-1-piperazineethanesulfonic acid, pH 7.4, 60 mM NaCl, 32 mM KCl, 3 mM Na_2HPO_4, 5 mM $MgCl_2$, 2 mM levamisole, 0.1% tricaine, 1 µM LysoTracker Red DND-99) and examined by fluorescence microscopy.

Microscopy

Nomarski and fluorescence images were obtained with a Zeiss Axio Imager M1 microscope system equipped with AxioVision software (Zeiss, Jena, Germany). Confocal images were acquired with a Nikon ECLIPSE TE2000-E (Nikon, Melville, NY) equipped with a CSU10 (Yokogawa, Tokyo, Japan)/iXon DV887 (Andor, Belfast, United Kingdom) confocal scanner unit and processed with Nikon NIS-Elements AR3.2, ImageJ (National Institutes of Health, Bethesda, MD), and

Photoshop (Adobe, San Jose, CA) software. For quantification of the fluorescence intensity of GFP on phagosomes, the area of the limiting phagosomal membrane in each image was selected manually using ImageJ software, and the fluorescence intensity in the selected area was measured.

RNA interference experiments

The *C. elegans* open reading frame–RNA interference (RNAi) library, version 1.1, was purchased from Open Biosystems (Huntsville, AL). The feeding RNAi protocol was performed as described previously (Kamath *et al.*, 2001; Poteryaev *et al.*, 2007). Briefly, adult animals (P0) were placed on RNAi plates, and F1 adult animals were observed. The animals were maintained at 20°C during RNAi treatment.

In vitro pull-down assay

Flag-tagged ARL-8 (Flag-ARL-8) was produced in the *Escherichia coli* strain BL21-CodonPlus (DE3)-RIL (Agilent Technologies, Santa Clara, CA) using pCold TF expression vector (Takara Bio, Otsu, Japan). cDNA encoding *vps-41* (isoform a) was subcloned into pMyc-CMV5 vector, and the expression vector was transfected into HEK293T cells using Lipofectamine2000 (Life Technologies, Carlsbad, CA). The transfected cells were homogenized 24 h after transfection in buffer A (10 mM triethanolamine-acetic acid, pH 7.6, 250 mM sucrose and 1 mM EDTA) and centrifuged (200,000 × *g*, 30 min, 4°C). The supernatant was mixed with purified Flag-ARL-8 proteins that had been preloaded with GDP or GTPγS and bound to anti–Flag M2 agarose (Sigma-Aldrich, St. Louis, MO), and the mixture was incubated for 1.5 h at 4°C in buffer B (37 mM Tris-HCl, pH 7.5, 2.6 mM triethanol amine-acetic acid, pH 7.6, 74 mM NaCl, 65 mM sucrose, 3.7 mM $MgCl_2$, 0.26 mM EDTA, 0.74 mM dithiothreitol [DTT], 2.22 mM dimyristoylphosphatidyl choline [DMPC], 0.37 mM 4-(2-aminoethyl) benzenesulfonyl fluoride hydrochloride, and 3.7 μM GDP or GTPγS). Anti-Flag M2 agarose in the mixture was then washed three times with buffer C (50 mM Tris-HCl, pH 7.5, 100 mM NaCl, 5 mM $MgCl_2$, 1 mM DTT, 3 mM DMPC, and 5 μM GDP or GTPγS), followed by incubation with Flag peptide (200 μg/ml; Sigma-Aldrich) for 30 min at 4°C. The Flag-peptide eluted fraction was subjected to Western blot analysis using anti-Myc and anti-Flag antibodies.

ACKNOWLEDGMENTS

We gratefully acknowledge R. Y. Tsien for the mCherry plasmids, X. Wang for *qxIs58*[$P_{ced\text{-}1}$*::lmp-1::Cherry*], and present and former members of the Katada laboratory for useful discussions. Some strains were provided by the CGC, which is funded by the National Institutes of Health Office of Research Infrastructure Programs (P40 OD010440). This work was supported in part by research grants from the Ministry of Education, Culture, Sports, Science and Technology of Japan and the Japan Society for the Promotion of Science (in both cases to K.K., K.S., M.F., T.K., K.G.-A., and S.M.) and the Japan Science and Technology Agency (to K.G.-A. and S.M.)

REFERENCES

Akbar MA, Tracy C, Kahr WH, Kramer H (2011). The full-of-bacteria gene is required for phagosome maturation during immune defense in *Drosophila*. J Cell Biol 192, 383–390.

Bagshaw RD, Callahan JW, Mahuran DJ (2006). The Arf-family protein, Arl8b, is involved in the spatial distribution of lysosomes. Biochem Biophys Res Commun 344, 1186–1191.

Brenner S (1974). The genetics of *Caenorhabditis elegans*. Genetics 77, 71–94.

Desjardins M, Huber LA, Parton RG, Griffiths G (1994). Biogenesis of phagolysosomes proceeds through a sequential series of interactions with the endocytic apparatus. J Cell Biol 124, 677–688.

Duclos S, Diez R, Garin J, Papadopoulou B, Descoteaux A, Stenmark H, Desjardins M (2000). Rab5 regulates the kiss and run fusion between phagosomes and endosomes and the acquisition of phagosome leishmanicidal properties in RAW 264.7 macrophages. J Cell Sci 113, 3531–3541.

Elliott MR, Ravichandran KS (2010). Clearance of apoptotic cells: implications in health and disease. J Cell Biol 189, 1059–1070.

Epp N, Rethmeier R, Kramer L, Ungermann C (2011). Membrane dynamics and fusion at late endosomes and vacuoles—Rab regulation, multisubunit tethering complexes and SNAREs. Eur J Cell Biol 90, 779–785.

Fadeel B (2003). Programmed cell clearance. Cell Mol Life Sci 60, 2575–2585.

Fadok VA, Bratton DL, Rose DM, Pearson A, Ezekewitz RA, Henson PM (2000). A receptor for phosphatidylserine-specific clearance of apoptotic cells. Nature 405, 85–90.

Garg S, Sharma M, Ung C, Tuli A, Barral DC, Hava DL, Veerapen N, Besra GS, Hacohen N, Brenner MB (2011). Lysosomal trafficking, antigen presentation, and microbial killing are controlled by the Arf-like GTPase Arl8b. Immunity 35, 182–193.

Gumienny TL, Lambie E, Hartwieg E, Horvitz HR, Hengartner MO (1999). Genetic control of programmed cell death in the *Caenorhabditis elegans* hermaphrodite germline. Development 126, 1011–1022.

Guo P, Hu T, Zhang J, Jiang S, Wang X (2010). Sequential action of *Caenorhabditis elegans* Rab GTPases regulates phagolysosome formation during apoptotic cell degradation. Proc Natl Acad Sci USA 107, 18016–18021.

Henry RM, Hoppe AD, Joshi N, Swanson JA (2004). The uniformity of phagosome maturation in macrophages. J Cell Biol 164, 185–194.

Hofmann I, Munro S (2006). An N-terminally acetylated Arf-like GTPase is localised to lysosomes and affects their motility. J Cell Sci 119, 1494–1503.

Kamath RS, Martinez-Campos M, Zipperlen P, Fraser AG, Ahringer J (2001). Effectiveness of specific RNA-mediated interference through ingested double-stranded RNA in *Caenorhabditis elegans*. Genome Biol 2, RESEARCH0002.

Kaniuk NA *et al.* (2011). *Salmonella* exploits Arl8B-directed kinesin activity to promote endosome tubulation and cell-to-cell transfer. Cell Microbiol 13, 1812–1823.

Kinchen JM, Cabello J, Klingele D, Wong K, Feichtinger R, Schnabel H, Schnabel R, Hengartner MO (2005). Two pathways converge at CED-10 to mediate actin rearrangement and corpse removal in *C. elegans*. Nature 434, 93–99.

Kinchen JM, Doukoumetzidis K, Almendinger J, Stergiou L, Tosello-Trampont A, Sifri CD, Hengartner MO, Ravichandran KS (2008). A pathway for phagosome maturation during engulfment of apoptotic cells. Nat Cell Biol 10, 556–566.

Kinchen JM, Ravichandran KS (2008). Phagosome maturation: going through the acid test. Nat Rev Mol Cell Biol 9, 781–795.

Kinchen JM, Ravichandran KS (2010). Identification of two evolutionarily conserved genes regulating processing of engulfed apoptotic cells. Nature 464, 778–782.

Klassen MP *et al.* (2010). An Arf-like small G protein, ARL-8, promotes the axonal transport of presynaptic cargoes by suppressing vesicle aggregation. Neuron 66, 710–723.

Lettre G, Hengartner MO (2006). Developmental apoptosis in *C. elegans*: a complex CEDnario. Nat Rev Mol Cell Biol 7, 97–108.

Liu QA, Hengartner MO (1998). Candidate adaptor protein CED-6 promotes the engulfment of apoptotic cells in *C. elegans*. Cell 93, 961–972.

Lu Q, Zhang Y, Hu T, Guo P, Li W, Wang X (2008). *C. elegans* Rab GTPase 2 is required for the degradation of apoptotic cells. Development 135, 1069–1080.

Mangahas PM, Yu X, Miller KG, Zhou Z (2008). The small GTPase Rab2 functions in the removal of apoptotic cells in *Caenorhabditis elegans*. J Cell Biol 180, 357–373.

Mello CC, Kramer JM, Stinchcomb D, Ambros V (1991). Efficient gene transfer in *C. elegans*: extrachromosomal maintenance and integration of transforming sequences. EMBO J 10, 3959–3970.

Mitani S (1995). Genetic regulation of *mec-3* gene expression implicated in the specification of the mechanosensory neuron cell types in *Caenorhabditis elegans*. Develop Growth Differ 37, 551–557.

Mrakovic A, Kay JG, Furuya W, Brumell JH, Botelho RJ (2012). Rab7 and Arl8 GTPases are necessary for lysosome tubulation in macrophages. Traffic 13, 1667–1679.

Nakae I, Fujino T, Kobayashi T, Sasaki A, Kikko Y, Fukuyama M, Gengyo-Ando K, Mitani S, Kontani K, Katada T (2010). The Arf-like GTPase Arl8 mediates delivery of endocytosed macromolecules to lysosomes in *Caenorhabditis elegans*. Mol Biol Cell 21, 2434–2442.

Nickerson DP, Brett CL, Merz AJ (2009). Vps-C complexes: gatekeepers of endolysosomal traffic. Curr Opin Cell Biol 21, 543–551.

Nishikiori M, Mori M, Dohi K, Okamura H, Katoh E, Naito S, Meshi T, Ishikawa M (2011). A host small GTP-binding protein ARL8 plays crucial roles in tobamovirus RNA replication. PLoS Pathog 7, e1002409.

Poteryaev D, Fares H, Bowerman B, Spang A (2007). *Caenorhabditis elegans* SAND-1 is essential for RAB-7 function in endosomal traffic. EMBO J 26, 301–312.

Reddien PW, Horvitz HR (2004). The engulfment process of programmed cell death in *Caenorhabditis elegans*. Annu Rev Cell Dev Biol 20, 193–221.

Roberts EA, Chua J, Kyei GB, Deretic V (2006). Higher order Rab programming in phagolysosome biogenesis. J Cell Biol 174, 923–929.

Rosa-Ferreira C, Munro S (2011). Arl8 and SKIP act together to link lysosomes to kinesin-1. Dev Cell 21, 1171–1178.

Seto S, Tsujimura K, Koide Y (2011). Rab GTPases regulating phagosome maturation are differentially recruited to mycobacterial phagosomes. Traffic 12, 407–420.

Vieira OV, Botelho RJ, Grinstein S (2002). Phagosome maturation: aging gracefully. Biochem J 366, 689–704.

Vieira OV, Bucci C, Harrison RE, Trimble WS, Lanzetti L, Gruenberg J, Schreiber AD, Stahl PD, Grinstein S (2003). Modulation of Rab5 and Rab7 recruitment to phagosomes by phosphatidylinositol 3-kinase. Mol Cell Biol 23, 2501–2514.

Wang X *et al*. (2003). Cell corpse engulfment mediated by *C. elegans* phosphatidylserine receptor through CED-5 and CED-12. Science 302, 1563–1566.

Wickner W (2010). Membrane fusion: five lipids, four SNAREs, three chaperones, two nucleotides, and a Rab, all dancing in a ring on yeast vacuoles. Annu Rev Cell Dev Biol 26, 115–136.

Wu YC, Horvitz HR (1998). The *C. elegans* cell corpse engulfment gene ced-7 encodes a protein similar to ABC transporters. Cell 93, 951–960.

Wu YC, Stanfield GM, Horvitz HR (2000). NUC-1, a *Caenorhabditis elegans* DNase II homolog, functions in an intermediate step of DNA degradation during apoptosis. Genes Dev 14, 536–548.

Xiao H, Chen D, Fang Z, Xu J, Sun X, Song S, Liu J, Yang C (2009). Lysosome biogenesis mediated by vps-18 affects apoptotic cell degradation in *Caenorhabditis elegans*. Mol Biol Cell 20, 21–32.

Yu X, Lu N, Zhou Z (2008). Phagocytic receptor CED-1 initiates a signaling pathway for degrading engulfed apoptotic cells. PLoS Biol 6, e61.

Zhou Z, Hartwieg E, Horvitz HR (2001). CED-1 is a transmembrane receptor that mediates cell corpse engulfment in *C. elegans*. Cell 104, 43–56.